Original Article

Spatial structure of precipitation in the Brazilian Amazonia: geostatistics with block kriging

**Humberto Millán-Vega [1] *, Jakeline Rabelo-Lima [1],
Nathalí Valderá-Figueredo [2]**

[1]Amazonas State University, Physics Collegiate, Center for Superior Studies of Tefé, Brazil.
[2]Instituto de Meteorología, La Habana, Cuba

https://eqrcode.co/a/PGTZnx

ABSTRACT: The Geostatistical analysis is an important tool for identifying distances over which rainfall shows spatial correlation. The objectives of the present work are: to model the spatial structure of rainfall patterns in the Brazilian rainforest using three timescales and to assess kriging interpolation for predicting rainfall data at ungauged sites. We used Geostatistical modeling combined with block kriging. The rainfall data were collected from 218 rain gauges corresponding to 64 municipalities located within 9 Amazonia states. Data corresponded to monthly mean rainfall and annual rainfall computed from historical records. The last date for data collection was December 2015. Three timescales were considered: months with minimum and maximum rainfall, January-June and July-December time periods and annual rainfall. The spherical model fitted reasonably well the semivariograms corresponding to March and January-June, the Gaussian model fitted quite well the semivariograms corresponding to September and July-December periods while the exponential model fitted the annual rainfall. The cross-validation analyses based on Mean Absolute Error and goodness-of-prediction statistics showed that kriged values (kriging maps) could be better predictors of rainfall for areas without rain gauges (unsampled zones) than mean rainfall values computed from adjacent sampled areas. It was found a significant negative statistical relationship between forest loss and rainfall occurrence which confirms the influence of deforestation on the hydrology of the Amazon basin.

Key words: Amazonian Rainforest, Geostatistics, Spatial Variability, Hydrology.

INTRODUCTION

The Amazonian rainforest is connected to the global hydrological cycle (Yoon & Zeng, 2010). Deforestation so as intense fires are factors affecting rainfall distribution and the Amazonian climate in general (Coe et. al., 2013). Bonini et. al. (2014) found negative correlations between deforestation and rainfall in Mato Grosso. Some studies have shown a decrease in regional evapotranspiration and precipitation due to increase in surface temperature associated to large-scale deforestation (Sellers et. al., 1997). This alters the hydrological cycle and influences the regional climate (Bagley et. al., 2014). Debortoli et. al. (2015) found that the rainy season was shorter at 88 % of the 200 observed rain gauges. Rainfall occurrence at the Northeast and the Southern regions of Brazil is influenced by the seasonal displacement of the Intertropical Convergence Zone and the South Atlantic Convergence Zone (Marengo et. al., 2011).

Rainfall variability in the Amazonia is correlated with the sea surface temperature patterns in the Atlantic and Pacific oceans during December, January and February (Martins *et. al.*, 2015). The reality is complex since past investigations have shown a decadal intensification of rainfall over the whole Amazon basin (Chen *et. al.*, 2002). The vulnerability of the region could be clear by the fact that Amazonia experienced its worst drought events in 2005 and 2010 (Davidson *et. al.*, 2012). However, it has been hypothesized that a physical mechanism of forest-induced atmospheric circulation called biotic pump by Makarieva & Gorshkov (2007) was responsible of the Amazonian forests greened-up during that 2005 drought (Saleska *et. al.*, 2007).

Costa *et. al.* (2008) used geostatistical methods for analyzing precipitation extremes in Southern Portugal while Sarangui *et. al.* (2015) mapped the rainfall variability over the island of St. Lucia. In general, geostatistical analysis of climatic variables has been very difficult to perform due, in part, to the limited availability of measurement points which affects the estimation at ungauged sites (Sarangi *et. al.*, 2005). Webster & Oliver (1992) demonstrated that at least 150 spatial points (e.g. rain gauges or meteorological stations) are required for a reliable geostatistical analysis. Once this problem has been solved, an appropriate kriging estimator (Burgess & Webster, 1980) could be a valuable tool for predicting rainfall data at ungauged sites. The spatial variability of precipitation also controls the spatial variation of other variables such as evapotranspiration and water storage. Due to the environmental significance of the Amazonian basin, the analysis of the spatial distribution of rainfall patterns is essential for agricultural, engineering and ecological planning. The objectives of the present work are to model the spatial structure of rainfall patterns in the Brazilian rainforest using three timescales and to search for any statistical relationship between deforestation and rainfall occurrence.

MATERIALS AND METHODS

Study area and rainfall data

The present study spanned 64 municipalities corresponding to 9 Amazonian states from Brazil. The geographical zone covered approximately from 5.03 ºN to 16.45 ºS and 42.83 to 70.93 ºW. Rainfall data refer to historical monthly mean and annual records collected from 218 rain gauges (Figure 1).
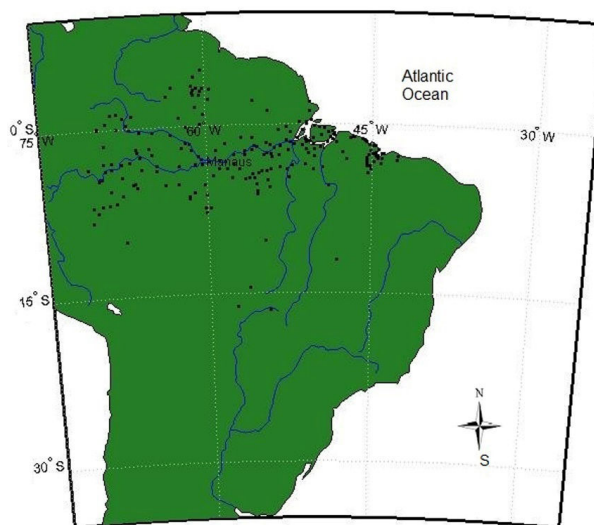

Figure 1. Study region and rain gauge locations.

The records ranged from the last 16 years for Rondonopolis (Mato Grosso state) to the last 106 years for Manaus (Amazonas state). The last date for data collection was December 2015. Three timescales were considered: individual months with minimum (September) and maximum (March) rainfall, January-June (rainy season), July-December (dry season) and annual rainfall. Note that January-June and July-December overlap winter and summer periods. However, our main goal was to establish a 6-month timescale separating wet and dry seasons.

Deforestation data

We performed an analysis on the potential relationship between the deforestation index and the annual rainfall including all the Amazon states. Most investigations try to search for relationships

between deforested areas (km^2) and rainfall. From our point of view that approach could be fictitious in this case as different states have different spatial extensions. We used instead the percentage of forest loss which relates forest loss (ha) to the total forest area (ha) for a particular site or state. The forest loss percentages are available at http://www.mongabay.com for 2001-2012 period (Butler, 2014). With that proposal, we averaged the available historical annual rainfall record for each studied Amazonian state and correlated them with the corresponding forest loss index.

Theoretical background on Geostatistics

Geostatistics incorporates the spatial coordinates of observations (x, y) in data processing. It is fundamental for the modeling of spatial patterns, prediction at unsampled points and estimation of the uncertainty inherent to those predictions (Goovaerts, 1998). The semivariance function, $\gamma(h)$, is one of the key components of geostatistics as it summarizes the spatial variation of the studied variable.

$$\gamma(h) = \frac{1}{2N(h)}\sum_{i=1}^{N(h)}\{z(x_i) - z(x_i + h)\}^2 \quad (1)$$

Where $\gamma(h)$ is the value of the experimental semivariance at each separation distance (lag), h, N(h) is the number of data pairs separated by the lag h, $z(x_i)$ and $z(x_i + h)$ are the rainfall values at location x_i and $x_i + h$, respectively. A plot of ((h) versus h defines the experimental semivariogram. Different models are available for fitting the experimental semivariogram (see for instance McBratney & Webster, 1986). We explored three transitive models (spherical, exponential and Gaussian models).

$$\begin{cases} \gamma(h) = C_0 + C\left[\frac{3}{2}\left(\frac{h}{A_0}\right) - \frac{1}{2}\left(\frac{h}{A_0}\right)^3\right] & for\ h \leq A_0 \\ \gamma(h) = C_0 + C & for\ h > A_0 \end{cases} \quad (2)$$

Equation (2) represents the spherical isotropic model. In this case C_0 is the nugget variance or nugget effect ($C_0 \geq 0$), C is the structural variance ($C \geq C_0$), $C_0 + C$ is the upper limit of the semivariogram (sill) and A_0 is the distance at which semivariogram reaches a constant semivariance

value (correlation range parameter). The Spatial Dependence Degree Index ($SDDI$) can be computed as the ratio between the structural variance, C , which characterizes the variance accounted for by the spatial dependence and the sill, $C_0 + C$. For example, $SDDI < 0.25$ suggests weak spatial dependence, $0.25 < SDDI < 0.75$ corresponds to moderate spatial dependence while $SDDI > 0.75$ indicates strong spatial dependence. This is a modification to the ratio nugget/sill variance proposed by Cambardella *et. al.* (1994). The range is the limit of spatial dependence. The spherical model characterizes a moving average of a randomized process (Kuzyakova *et. al.* 2001).

$$\gamma(h) = C_0 + C\left[1 - exp\left(-\frac{h}{A_0}\right)\right] \quad (3)$$

Equation (3) is the isotropic exponential model. It differs from the spherical model in the rate at which the sill is reached. It represents autoregressive processes of first order (e.g. Markov or Poisson processes) as the autocorrelation function decays exponentially (Wang *et. al.* 2010).

$$\gamma(h) = C_0 + C\left[1 - exp\left(-\frac{h}{A_0}\right)^2\right] \quad (4)$$

Equation (4) corresponds to the Gaussian or hyperbolic isotropic model. It is almost similar to the exponential model but the departure from the nugget variance is smoother.

Block Kriging

Block kriging is a robust interpolation method for estimating values of the variable (e.g. rainfall values in this case) at ungauged zones (Burguess & Webster, 1980). The block kriging estimator (Z_S) of the average rainfall on a given zone (S) is built as a linear combination of the available rainfall data:

$$Z_S^* = \sum_{i=1}^{n}\lambda_i Z_i \quad (5)$$

Where Z_S^* is the estimated kriged value of Z in the area S and λ_i are weighing factors such that:

$$\sum_{i=1}^{n}\lambda_i = 1 \quad (6)$$

In this case n is the number of rainfall values in the vicinity of Z_S^* . The block kriging estimation is unbiased under the condition:

$$E[Z_S^* - Z_S] = 0 \quad (7)$$

That is, the mathematical expectation of Z_S^* is the same as that of the real Z_S value.

The accuracy of rainfall maps was assessed through a cross-validation process (Davis, 1987). The agreement between estimated and measured values was quantified using mean absolute error (MAE hereafter) (Voltz & Webster, 1990) and goodness-of-prediction statistics (G statistics hereafter) (Agterberg, 1984). The MAE statistics is in fact a residual sum:

$$MAE = \frac{1}{N} \sum_{i=1}^{N} (|z(x_i) - \hat{z}(x_i)|) \quad (8)$$

Where $\hat{z}(x_i)$ is the predicted rainfall value at location i.

The G statistics is a sort of balance between kriging and sample mean as potential rainfall predictors:

$$G = \left(1 - \frac{\sum_{i=1}^{N} [z(x_i) - \hat{z}(x_i)]^2}{\sum_{i=1}^{N} [z(x_i) - z(mean)]^2} \right) \quad (9)$$

Where $z(mean)$ is the mean value of all the observations.

Equation (9) defines three possibilities:

i. $G = 0$ indicates that kriged values or sample mean could be used as rainfall predictors,

ii. $G < 0$ suggests that sample mean is a better predictor than kriging,

iii. $G > 0$ indicates that kriging is more appropriate than sample mean for making reliable predictions at ungauged sites.

It is useful to recall that due to earth curvature the use of geographical coordinates for large scale spatial analysis is inappropriate. Thus, in order to perform the spatial analysis, geographical coordinates were transformed into rectangular (x, y) coordinates.

Standard statistics and Geostatistical computation

Classical statistics (e.g. first and second order statistics and test of normality) and linear regression analysis were conducted using the Statistica™ Software Package (StatSoft. Inc., 2011). All the geostatistical analyses were performed using the GS+ Geostatistical Software Package (Gamma Design Software, 2001). In particular, we set the minimum lag class distance to 247.25 km. Block kriging estimation was carried out using 4 x 4 local grids and 16 neighbors within a radius equal to the range of the semivariogram. We selected a total of six map contour levels.

RESULTS AND DISCUSSION

March and September were the months with maximal and minimum rainfall values, respectively. Those months also showed the maximum and minimum standard deviation values (117 mm and 60 mm, respectively) (Table 1).

The spatial distribution of rainfall based on upper thresholds is highly variable in the whole region (Figure 2A-E). The maximal historical annual rainfall (4253 mm) as represented by the upper threshold was located in Fonte Boa (Amazonian state, 2.35 ºS, 65.12 ºW) while the minimum upper threshold of annual rainfall (1980 mm) was recorded at Caceres (Mato Grosso state, 16.05 ºS, 57.68 ºW) (Figure 2E).

Some selected areas from different states like Manaus (3.1 ºS, 60.01 ºW, Amazonas state), Caceres (16.05 ºS, 57.68 ºW, Mato Grosso state), Boa Vista (2.82 ºN, 60.66 ºW, Roraima state), Macapá (0.1 ºS, 51.1 ºW, Amapá state) and Rio Branco (9.96 ºS, 67.8 ºW, Acre state) showed different behavior of rainfall occurrence along the year (Figure 3).

Despite the fact that some rainfall records did not fit the normality condition (January, February, April, July, August, October and November), the data sets of our interest (March, September, January-June, July-December and annual rainfall) did not differ statistically from normality according to the Kolmogorov-Smirnov and Lilliefors test for normality at $p < 0.05$ (Table 1). This is a basic condition for geostatistical analysis as one could assume stationarity of the second order. That is, the expectation value and the spatial covariation $C(h)$ can be considered as constant.

Table 1. Descriptive statistics of monthly, six month and annual rainfall. KSL is Kolmogorov-Smirnov and Lilliefors test for normality. NS means that Rainfall distribution does not differ statistically from normality at $p < 0.05$.

Month	Mean (mm)	Min. (mm)	Max. (mm)	Std.Dev	CV (%)	KSL
Jan	243	13	563	94	39	0.075
Feb	269	13	621	106	39	0.108
Mar	313	26	756	117	37	NS
Apr	301	47	579	95	31	0.075
May	261	5	655	86	33	NS
Jun	179	3	438	93	52	NS
Jul	138	6	374	84	61	0.086
Aug	104	5	378	69	66	0.134
Sep	90	2	283	60	66	NS
Oct	104	2	358	75	71	0.111
Nov	124	4	333	79	63	0.106
Dec	174	18	392	85	49	NS
Jan-Jun	1569	450	3254	432	28	NS
Jul-Dec	735	131	1887	342	46	NS
Annual	2303	1226	4253	560	24	NS

The selected Geostatistical models described reasonably well the experimental semivariograms. The Gaussian model fitted quite well September ($R = 0.988$) and July-December ($R = 0.991$) rainfall data (Figure 4B and D) while the spherical model was the best choice for describing the spatial structure of rainfall for March, January-June and annual periods (Figure 4A, C and E) with correlation ranges of 1521 km, 1110 km and 1020 km, respectively (Table 2).

The interpolation (kriging) maps corresponding to March and September agreed approximately well with the results shown in Figure 3 in terms of maximal monthly rainfall values (Figure 5A and B). In all cases, central Amazonia was the region with less rainfall occurrence. The January-June (wet season) kriging map identified reasonably well the region with rainfall values over 1569 mm (mean value of the 6-month period) at the Northern to Northeast Amazonia (Figure 5C). The interpolation map for the July-December time period (dry season) located the maximum rainfall values at the West Amazonia, approximately (Figure 5D). However, maximal rainfall values at the Western Amazonia in July-December were smaller than those corresponding to Northern-

Northeast Amazonia. The kriging map corresponding to annual rainfall combined the spatial distribution of rainfall patterns in the whole studied region for the selected time scales (Figure 5E).

The MAE as a goodness-of-prediction statistics ranged from 27 mm for September to 346 mm for annual rainfall as expected. The positive value of G statistics indicates that kriging could be a better predictor of rainfall at ungauged sites than mean rainfall values. In particular, September and July-December (dry season) were the timescales where kriging interpolation performed better ($G = 0.627$ and $G = 0.700$, respectively). At the same time, the cross-validation process indicated that those timescales also rendered the best correlation coefficient between observed and predicted rainfall values ($R = 0.792$ and $R = 0.846$, respectively) (Table 3).

It is noted that rainfall records larger than mean values shifted from Northeast to Northwest Amazonia while rainfall values smaller than mean showed the reverse trend. This bias of rainfall has been well documented in the literature. For example, Martins *et. al.* (2015) have found that Atlantic and Pacific sea surface temperature (SST)
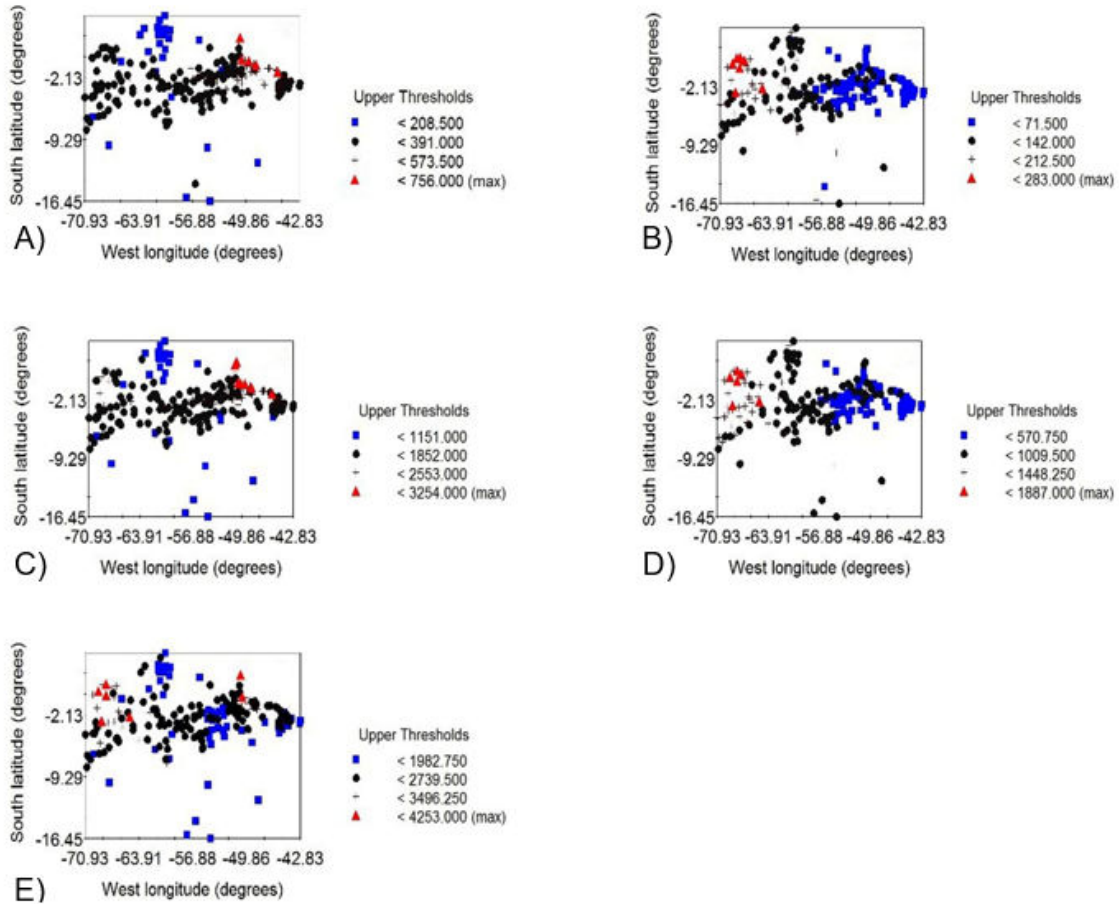
Figure 2. Rainfall distribution in the study region based on geographical coordinates: A) March, B) September, C) January-June, D) July-December and E) Annual.

modulate the Northern area of Amazonia during June-August period (winter season) while Pacific SST acts on the Eastern region during December-February period (summer season). It is very difficult to define wet and dry seasons within the Amazonian region. In winter (June-August period) an isobar of normal atmospheric pressure ($Pr = 1013.25 \ mb$) crosses over the Amazon rainforest from Northeast (Amapá state) to approximately Southwest (Acre state). This can produce a rainfall shortage in Macapá, Manaus and Rio Branco. That situation is reversed in summer (December-February period) due, in part, to the presence of a moderate low pressure zone ($Pr = 1009.25 \ mb$) in Northeast to central Amazonia approximately. That consideration

agrees well with a previous investigation by Chaves & Cavalcanti (2001).

The quasi-parabolic shape of the Gaussian model for lag distances near to the origin is indicative of a smooth spatial variability of rainfall in September and July-December. Such spatial organization held for a correlation length of about 1793 km (September) and 2044 km (July-December) with stronger spatial dependence in terms of *SDDI* (0.883 and 0.926 , respectively). Those larger correlation ranges suggest that rainfall events could be mainly of stratiform nature in September and July-December. It is known that stratiform precipitation is a large-scale process. That sort of seasonal range was previously discussed by van de Beek *et. al.* (2011) for the case of daily rainfall in The Netherlands.
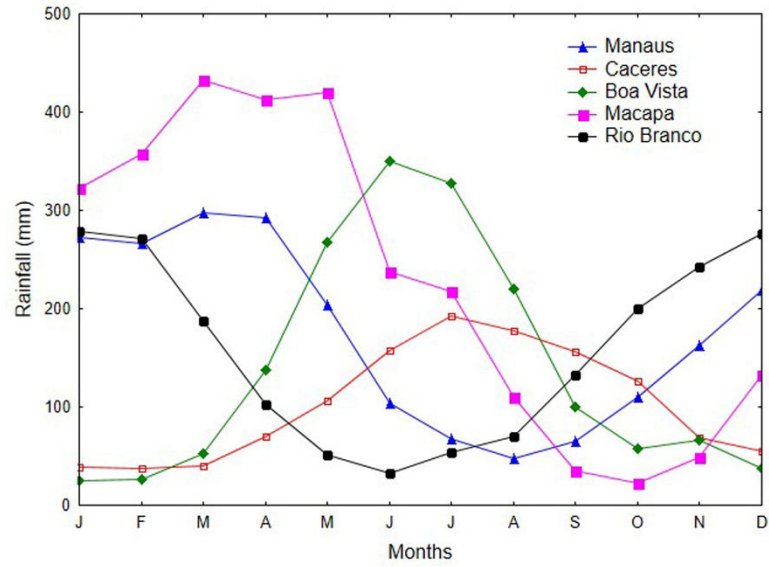
Figure 3. Monthly rainfall at five selected sites: Manaus (Amazonas state), Caceres (Mato Grosso state), Boa Vista (Roraima state), Macapá (Amapá state) and Rio Branco (Acre state).
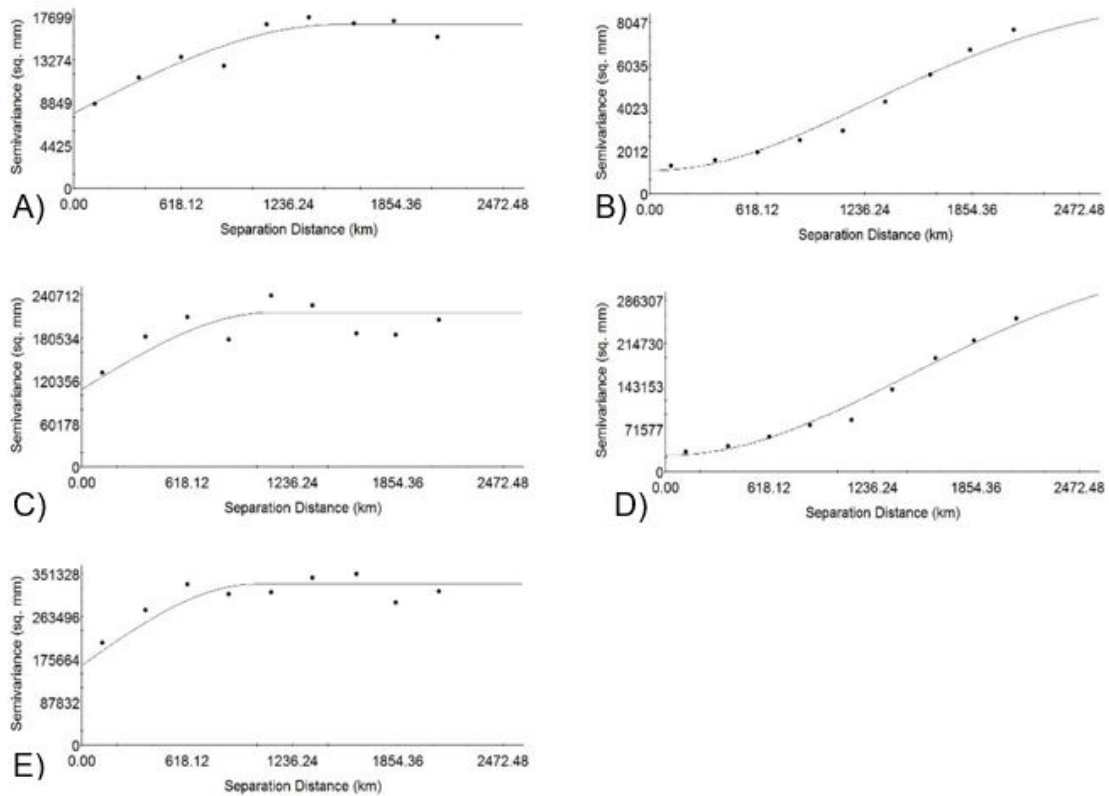

Figure 4. Univariate semivariogram for each selected rainfall period: A) March, B) September, C) January-June, D) July-December and E) annual.

Table 2. Parameters of the fitted geostatistical models (R is the correlation coefficient).

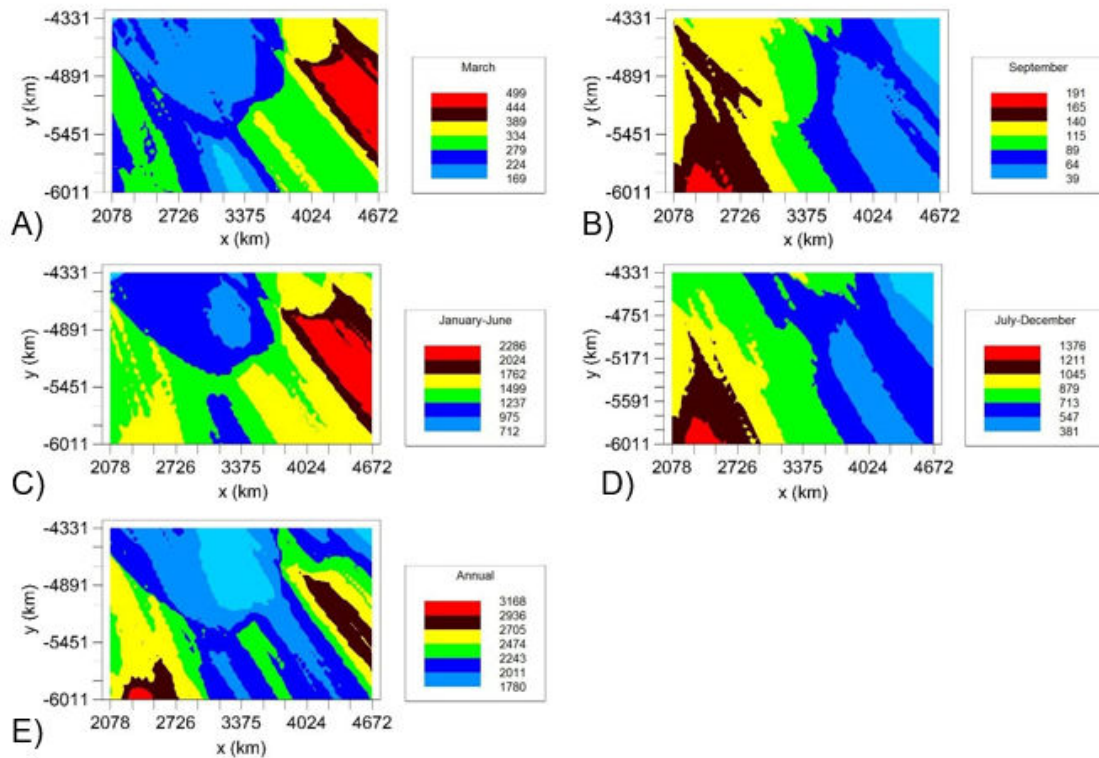| Period	Model	C_0 (mm²)	$C_0 + C$ (mm²)	A_0 (km)	$C/(C_0 + C)$	R
Mar	Spherical	7750	16930	1521	0.542	0.946
Sep	Gaussian	1080	9270	1793	0.883	0.988
Jan-Jun	Spherical	108200	216500	1110	0.500	0.730
Jul-Dec	Gaussian	27000	365000	2044	0.926	0.991
Annual	Spherical	163100	330000	1020	0.506	0.881

Figure 5. Kriging maps corresponding to each rainfall period: A) March, B) September, C) January-June, D) July-December and E) Annual.

The nugget semivariance (1080 mm² in September and 27000 mm² for July-December period) could be related to random spatial variability at distances smaller than or equal to the shortest lag class distance interval (e.g. 247.25 km in this study). At this stage one could assume that local factors such as patches of deforested areas can produce local variations of relative humidity, evaporation, evapotranspiration and/or atmospheric pressure which also contribute to such unexplained rainfall variability. Note that annual precipitation showed the smaller correlation range ($A_0 = 1020$ km). One could conjecture that, in average, annual rainfall in the Amazonian rainforest is due mainly to convective mechanisms. We support such an assumption taking into account that January-June period ($A_0 = 1110$ km) includes the 68.1 % of the annual precipitation. Adjusting previous interpretations by Jongman *et. al.* (1995), one could assume that the spherical model describes abrupt rainfall changes at unequal distances. The high value of the nugget effect (7750 mm² for March, 108200 mm² for January-June and 163000 mm² for annual periods) indicates, to some extent, a higher short-range spatial variability for distances smaller than 247.25

km. This also could be due to the local nature of most convective events which depend on the organization of mesoscale (eg. length scale(100 km) processes (Takemi, 2010).

Table 3. Goodness-of-prediction statistics through cross-validation (R is the correlation coefficient between actual and estimated rainfall).

Period	MAE (mm)	G (-)	R
Mar	69	0.358	0.615
Sep	27	0.627	0.792
Jan-Jun	273	0.260	0.557
Jul-Dec	138	0.700	0.846
Annual	346	0.336	0.584

Even though the spherical model fitted reasonably well the annual rainfall data, one can note some sort of alternating rainfall patterns from 824 km to 2060 km along the sill. According to Pendergrass *et. al.* (2016), General Circulation Models are unable to resolve with precision individual mesoscale rainfall events which produce a lack of knowledge of the effect of climate change on rainfall pattern organization. One of the first steps toward filling that gap was the investigation by Ferreira *et. al.* (2018) for the case of the Southeast United States. Those authors found that short simulations provided an initial inside but much more simulations are needed for an appropriate understanding of the changes of rainfall organization and intensity under a global warming perspective.

We highlighted two rainfall gradients in the kriging map corresponding to the historical annual rainfall. One rainfall gradient is oriented approximately from the drier central Amazonia (Pará state) to Northern-Northeast Amazonia (e.g. Amapá state) while the other rainfall gradient extent from South Amazonia (Mato Grosso state) to the Western Amazonia (e.g. near the border between Amazonas state and the Eastern region of Peru). That annual spatial variability in the

Northern and Western Amazonia has been previously discussed by Ronchail *et. al.* (2002) in terms of the Intertropical Convergence Zone displacement while Sheil & Murdiyarso (2009) stressed the influence of land surface, atmosphere, soil moisture and evapotranspiration on the hydrological processes in the Amazon basin at inter-annual and annual time scales. Even though any statistical parameter (e.g. *MAE* and/or *G* parameter) could support the suitability of kriging, one needs additional information on the reality of those interpolated patterns. For example, the kriging map for annual rainfall shows a tendency of rainfall to decrease from Northern-Northeast to approximately Southern Amazonia.

Makarieva *et. al.* (2009) investigated the relationship between rainfall versus distance from the ocean along a 2800 km transect across the Amazon rainforest. That transect was established from 0 ºS, 50 ºW (Amapá state) to 5 ºS, 75 ºW (western region of Amazonas state and eastern zone of Peru). Those authors did not find a significant statistical relationship between rainfall and distance from the ocean and concluded that rainfall did not decrease along 2800 km inland. In order to gain more understanding on the potential factors affecting the rainfall spatial distribution, we designed an irregular, almost similar, transect of 2708 km but it started at 0.1 ºS, 50 ºW (Amazon estuary, Amapá state) and concluded at 8.95 ºS, 72.8 ºW (Western region of Acre state) (Figure 6A). Similar to Makarieva *et. al.* (2009), we also did not find a significant statistical relationship between rainfall and distance from the Atlantic Ocean. Nevertheless, one can note a subtle trend to rainfall decline (Figure 6B). It is possible that only 17 sites are not enough and more data points are required for a reliable analysis. However, it is also likely that neither Makarieva *et. al.* (2009) transect nor our own transect crossed over the most deforested regions. This deserves more investigation in the future.
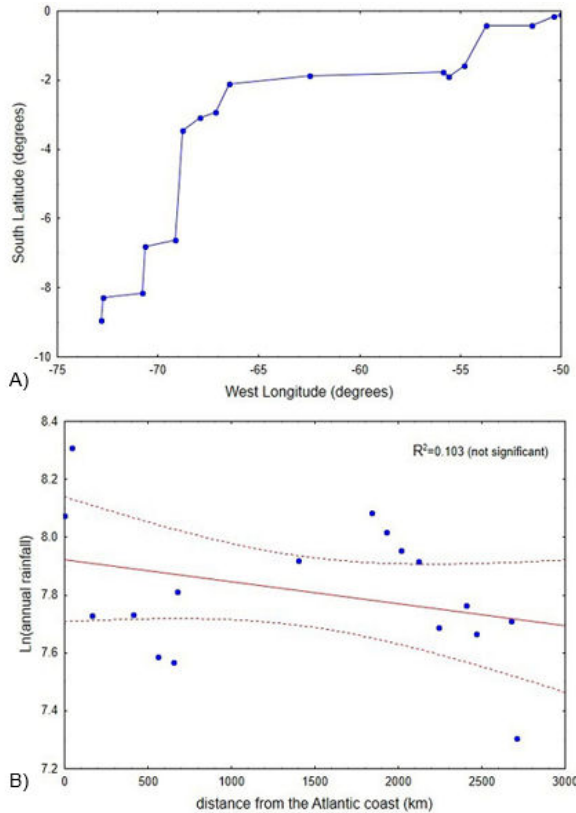
Figure 6. A) Irregular transect from the Atlantic coast (the starting point is the Amazon estuary, -0.1 ºS Latitude, -50.0ºW Longitude) and B) annual rainfall versus inland distance.

Deforestation as a man-induced factor can also influence the rainfall pattern organization and to modify the Amazonia hydrometeorology. This has been a controversial issue for many years. We found a significant negative linear relationship between the percentage of forest loss and annual rainfall ([Figure 7](#)).
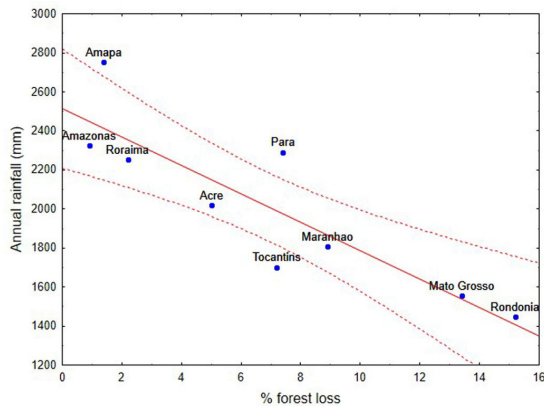

Figure 7. Deforestation versus historical annual rainfall.

CONCLUSIONS

- We have used geostatistical tools for investigating the actual spatial organization of rainfall patterns in the Brazilian Amazonia. Gaussian and spherical models captured approximately well the spatial structure of historical rainfall records.

- The parameters of the Geostatistical models could be related to the occurrence of convective or stratiform rainfall in different periods of the year.

- The interpolation maps showed a seasonal shift of maximal rainfall from Northern-Northeast to West Amazonia while the South-Central to South region remains drier. This agrees with the assumption of the Amazonian precipitation dipole previously investigated with simulation models.

- It was not found any consistent statistical relationship between rainfall and distance from the Atlantic coast. However, it was found a significant negative correlation between average rainfall computed for each state and forest loss as a deforestation index.

- Even though many investigations have been conducted, the influence of deforestation and land use change on the actual spatial structure of rainfall patterns deserves much more attention. Future models need to include spatial maps of deforestation and their influence on spatial patterns of rainfall.

REFERENCES

AGTERBERG, F.P. (1984): Trend surface analysis. In: Gaile, G.L; Willmot, C.J. (Ed.). Spatial statistics and models. Reidel, Dordrecht, The Netherlands, p. 147-171.

BAGLEY, J.E.; DESAI, A.R.; HARDING, K.J. & SNYDER, P.K. *et. al.* (2014): Drought and deforestation: has land cover change influenced recent precipitation extremes in the Amazon? *Journal of Climate*, 27: 345-361.

BONINI, I.; RODRIGUES, C.; DALLACORT, R. & MARIMON, B.H.Jr. *et. al.* (2014): Rainfall and deforestation in the municipality of Colíder, Southern Amazon. *Revista Brasileira de Meteorología*, 29: 483-493.

BURGESS, T.M. & WEBSTER, R. (1980): Optimal interpolation and isarithmic mapping of soil properties. II: Block kriging. *Journal of Soil Science*, 31:333-343.

BUTLER, R. (2014): Rainforest of Brazil: An Environmental Status Report ((2014): Rainforest of Brazil: An Environmental Status Report (http://www.mongabay.com). Accessed 30/11/2015.

CAMBARDELLA, C.A.; MOORMAN, T.B.; NOVAK, J.M. & PARKIN, T.B. *et. al.* (1994): Field-scale variability of soil properties in central Iowa soils. *Soil Science Society of America Journal*, 58: 1501-1511.

CHAVES, R.R. & CAVALCANTI, I.F.A. (2001): Atmospheric circulation features associated with rainfall variability over southern Northeast Brazil. *Monthly Weather Review*, 129: 2614-2626.

CHEN, J.; CARLSON, B.E. & DEL GENIO, A.D. (2002): Evidence for strengthening of the tropical circulation in the 1990s. Science, 295: 838-841.

COE, M.; MARTHEWS, T.R.; COSTA, M.H. & GALBRAITH, D. *et. al.* (2013): Deforestation and climate feedbacks threaten the ecological integrity of south-southeastern Amazonia. *Philosophical Transactions of the Royal Society B*, 368: 20120155.

COSTA, A.N.; DURÃO, R.; SOARES, A. & PEREIRA, M.J. (2008): A geostatistical exploratory analysis of precipitation extremes in Southern Portugal. *Statistical Journal*, 6: 21-32.

DAVIDSON, E.A.; DE ARAUJO, A.C.; ARTAXO, P. & BALCH, J.K. *et. al.* (2012): The Amazon basin in transition. *Nature*, 481: 321-328.

DAVIS, B.M. (1987): Uses and abuses of cross-validation in geostatistics. Mathematical Geology, 19: 241-248.

DEBORTOLI, N.S.; DUBREUIL, V.; FUNATZU, B. & DELAHAYE, F. *et. al.* (2015): Rainfall Patterns in the Southern Amazon: a chronological perspective (1971-2010). *Climate Change*, https://doi.org/10.1007/s10584015-1415-1.

FERREIRA, R.N.; NISSENBAUM, M.R. & RICKENBACH, T.M. (2018): Climate changes effects on summertime precipitation organization in the Southeast United States. *Atmospheric Research*, 214: 348-363.

GAMMA DESIGN SOFTWARE (2001): GS+ Geostatistics for the Environmental Sciences, version 5.1.1. Professional Edition, Plainwell, MI.

GOOVAERTS, P. (1998): Geostatistical tools for characterizing the spatial variability of microbiological and physic-chemical soil properties. *Biology and Fertility of Soils*, 27: 315-334.

JONGMAN, R.H.G.; TER BRAAK, C.J.F. & VAN TONGEREN, O.F.R. (1995): Data analysis in community and landscape ecology. Cambridge University Press, Cambridge, London.

KUZYAKOVA, I.F.; ROMANENKOV, V.A. & KUZYAKOV, Ya.V. (2001): Geostatistics in soil agrochemical studies. *Eurasian Soil* Science , 34: 1011-1017.

LLOPART, M.; REBOITA, M.S.; COPPOLA, E. & GIORGI, F. *et. al.* (2018): Land use change over the Amazon Forest and its impact on the local climate. *Water*, 10: 149.

MAKARIEVA, A.M. & GORSHKOV, V.G. (2007): Biotic pump of atmospheric moisture as driver of the hydrological cycle on land. *Hydrology and Earth System Sciences*, 11: 1013-1033.

MARENGO, J.; TOMASELLA, J.; ALVES, L.M. & SOARES, W.R. *et. al.* (2011): The drought of 2010 in the context of historical droughts in the Amazon region. *Geophysical Research Letters*, 38: L12703.

MARTINS, G., VON RANDOW, C.; SAMPAIO, G. & DOLMAN, A.J. (2015): Precipitation in the Amazon and its relationship with moisture

transport and tropical Pacific and Atlantic SST from the CMIP5 simulation. *Hydrology and Earth System Sciences* (Discussions), 12: 671-704.

MCBRATNEY, A.B. & WEBSTER, R. (1986): Choosing functions for semivariograms of soil properties and fitting them to sampling estimates. *Journal of Soil Science* , 37: 617-639.

PENDERGRASS, A.G.; REED, K.A. & MEDEIROS, B. (2016): The link between extreme precipitation and convective organization in a warming climate: global radiative-convective equilibrium simulations. *Geophysical Research Letters* , 43: 11445-11452.

RONCHAIL, J.; GERARD, C.; MOLINIER, M. & GUYOT, J.P. *et. al.* (2002): Interannual rainfall variability in the Amazon basin and sea-surface temperatures in the Equatorial Pacific and the Tropical Atlantic Oceans. *International Journal of Climatology*, 22: 1663-1686.

SALESKA, S.R.; DIDAN, K.; HUETE, A.R. & DA ROCHA, H.R. (2007): Amazon forests green-up during 2005 drought. Science , 318: 612.

SARANGI, A.; COX, C.A. & MADRAMOOTOO, C.A. (2005): Geostatistical methods for prediction of spatial variability of rainfall in a mountainous region. *Transactions of the American Society of Agricultural Engineers*, 48: 943-954.

SELLERS, P.J.; DICKINSON, R.E.; RANDALL, D.A. & BETTS, A.K *et. al.* (1997): Modeling the exchanges of energy, water, and carbon between continents and the atmosphere. Science , 275: 502-509.

SHEIL, D. & MURDIYARSO, D. (2009): How forests attract rain: an examination of a new hypothesis. *Bioscience*, 4: 341-347.

STATSOFT. INC. (2011): STATISTICA (Data Analysis Software System), version 10, Tulsa, OK.

TAKEMI, T. (2010): Dependence of the precipitation intensity in mesoscale convective systems to temperature lapse rate. *Atmospheric Research* , 96: 273-285.

VAN DE BEEK, C.Z.; LEIJNSE, H.; TORFS, P.J.J.F. & UIJLENHOET, R. (2011): Climatology of daily rainfall semi-variance in The Netherlands. *Hydrology and Earth System Sciences*, 15: 171-183.

WANG, G.; DOLMAN, A.J.; BLENDER, R. & FRAEDRICH, K. (2010): Fluctuation regimes of soil moisture in ERA-40 re-analysis data. *Theoretical and Applied Climatology*, 99: 1-8.

WEBSTER, R. & OLIVER, M.A. (1992): Sample adequately to estimate variograms of soil properties. *Journal of Soil Science* , 43: 177-192.

YOON, J.H.& ZENG, N. (2010): An Atlantic influence on Amazon rainfall. *Climate Dynamics*, 34: 249-264.